

Anna Harrison ORCID iD: 0000-0002-4752-5635

Running Head: Metal toxicity and groundwater-surface water interactions

Hyporheic interactions increase zinc exposure and effects to *Hyalella azteca* in sediments under flow-through conditions

Anna M. Harrison^{1,*}

Michelle L. Hudson¹

G. Allen Burton¹

¹School for Environment and Sustainability, University of Michigan, Ann Arbor, MI, USA

* Corresponding author (harri25a@cmich.edu)

Journal: Environmental Toxicology and Chemistry

Article Type: Environmental Toxicology (Original Article)

Acknowledgements – We thank the following lab staff for their support on this project:

Dr. Sara Nedrich, Alison Rentschler, Kesiree Thiamkeelakul, Yihan Li, Brianna

Westmoreland, and Tanner Hoag. This research was funded in part by the University of Michigan Graham Sustainability Institute and Rackham Graduate School.

This is the author manuscript accepted for publication and undergone full peer review but has not been through the copyediting, typesetting, pagination and proofreading process, which may lead to differences between this version and the [Version of Record](#). Please cite this article as [doi: 10.1002/etc.4554](https://doi.org/10.1002/etc.4554).

Data availability – Data and associated metal data are available from the corresponding author (harri25a@cmich.edu) or through the figshare online repository (doi: 10.6084/m9.figshare.8856260).

ABSTRACT

Groundwater-surface water interactions in the hyporheic transition zone can influence contaminant exposure to benthic macroinvertebrates. In streams, hyporheic flows are subject to varying redox conditions, which influence biogeochemical cycling and metal speciation. Despite these relationships, little is known about how these interactions influence ecological risk of contaminants. This study investigates the effects of hyporheic flows and zinc-contaminated sediments on the amphipod *Hyalella azteca*. Hyporheic flows were manipulated in laboratory streams during 10-day experiments. Zinc (Zn) toxicity was evaluated in freshly spiked and aged sediments. Hyporheic flows altered sediment and porewater geochemistry, oxidizing the sediments and causing changes to redox sensitive endpoints. Amphipod survival was lowest in the Zn sediment exposures with hyporheic flows. In freshly spiked sediments, porewater Zn drove mortality, while in aged sediments (SEM-AVS)/fOC influenced amphipod responses. This study highlights the important role of hyporheic flows in determining Zn bioavailability to benthic organisms and thereby can be important in ecological risk assessments.

Keywords: hyporheic zone, groundwater-surface water transition zone, sediment toxicity, metal bioavailability, environmental risk assessments

INTRODUCTION

Groundwater-surface water interactions influence most lotic ecosystems, but their effects on contaminant bioavailability remain largely unstudied. Previous work has demonstrated the importance of groundwater-surface water interactions in determining toxicity and bioaccumulation of chlorobenzenes for caged *Ceriodaphnia dubia*, *Hyaella azteca*, *Chironomus tentans* and *Lumbriculus variegatus* (Greenberg et al. 2002). The caged test organisms exposed to sediments had higher survival and lower chlorobenzene bioaccumulation at a site with downwelling hyporheic flow compared to sites without dominant hyporheic flow direction, despite higher porewater chlorobenzene concentrations at the downwelling site. Organism responses to chlorobenzene could not have been predicted without knowledge of these hyporheic flow conditions. As benthic macroinvertebrates are used to set standards for contaminant toxicity, a better understanding of effects from hyporheic flows is needed for risk assessments.

Ecological risk assessments for metals, in particular, may benefit from measurements of hyporheic flow, as hyporheic flows influence sediment redox chemistry and pH (Hendricks et al. 1993; Franken et al. 2001), which in turn affect metal speciation and binding (Calmano et al. 1993). In streams, upstream riffles are typically dominated by downwelling of surface waters into sediments and are more oxidized than downstream riffles, which are dominated by upwelling of more reduced hyporheic waters from the sediments (Boulton 1993; Brunke and Gonser 1997; Hendricks and White 2000; Olsen and Townsend 2003) (Figure 1).

Under physically and chemically stable conditions, divalent metals like Zinc (Zn) are likely to bind to various ligands in sediments, decreasing their bioavailability to biota.

The likelihood of ligand binding is related to the redox chemistry in the sediments. In anoxic sediments, sulfide is an important binding ligand. Organic carbon is an important binding ligand in both anoxic and oxic sediments (Calmano et al. 1993; Chapman et al. 1998). Iron and manganese oxide minerals offer a binding site for divalent metals under oxic conditions (Costello et al. 2015; Danner et al. 2015; Mendonca et al. 2017), which has been an important binding ligand in the hyporheic zone (Harvey and Fuller 1998). Thus, sulfide and organic carbon may be important binding ligands in more reduced upwelling zones, whereas iron and manganese oxide complexes may be a critical binding ligand in oxidized sediments characteristic of downwelling zones.

Despite evidence of the importance of hyporheic flows on contaminant exposure to benthic macroinvertebrates and ecological risk, hyporheic zones are generally unaccounted for in ecological risk assessments. Field research has demonstrated some effects of hyporheic flows on metal contaminant exposure and effects. Microbial communities of the hyporheic zone in mining impacted streams exhibited effects from metals on functional group structure (Feris et al. 2003; Feris et al. 2009). Macroinvertebrate communities were most diverse in metal-contaminated field sediments that had high hydraulic conductivity and high filtration of surface water into the streambank, essentially diluting metals within the hyporheic zone sediments (Gibert et al. 1995), similar to the relationship between chlorobenzene and downwelling observed in Greenberg et al. (2002). Macroinvertebrate communities in the hyporheic zone also responded to metal contamination (Nelson and Roline 1999; Moldovan et al. 2011), but research is limited that mechanistically links hyporheic flows to metal concentrations and biotic effects.

To assess the impacts of hyporheic flows in metal-contaminated sediment, artificial stream experiments in the laboratory can assist with understanding metal exposure and effects under controlled conditions. By eliminating many confounding variables present in the field, laboratory experiments can identify mechanisms of effects between physical processes, sediment chemistry and biological endpoints. Laboratory flume experiments showed effects of passive hyporheic flows on metal chemistry (Zaramella et al. 2006) and the effects of sedimentation on interstitial spaces in the hyporheic zone (Rehg et al. 2005). Mesocosm experiments also showed the importance of both upwelling and downwelling zones for amphipod presence in systems with excess sedimentation (Mathers et al. 2014). This body of work has indicated the importance of hyporheic flows on both metals and invertebrates, yet there is limited research to connect sediment metal chemistry to ecological effects in the hyporheic zone.

Our study assesses the influences of oxidized hyporheic flows on Zn bioavailability and effects to *H. azteca* in Zn amended sediment. We hypothesize that oxidized hyporheic flows will release more bound Zn from sediments, compared to exposures without hyporheic flow. Zn release will increase exposure and potentially cause adverse effects on *H. azteca*. We also hypothesize that over time Zn concentrations will stabilize and become less toxic to *H. azteca*.

METHODS

Sediment selection and spiking

Sediment was collected from an upstream reference reach of Little Black Creek (LBC) in Muskegon Heights, MI (43.216062 N, 86.180030 W). The outlet of LBC is a

U.S. EPA Area of Concern due to metal contamination from a Zn smelting operation (Cooper et al. 2001; Steinman et al. 2003), with documented concentrations above probable effects concentrations (PEC) (MacDonald et al. 2000). The sediment is sandy, allowing for hyporheic exchange during the mesocosm experiments. LBC sediment is low in sulfide and organic carbon and has moderate to high iron concentrations (Table 1). Sediment was collected from LBC and purged with N₂ gas before being sealed and stored for one month. Half of the sediment was amended with Zinc Chloride (ZnCl₂), to obtain total Zn concentrations above the PEC for Zn (459 mg/kg). Once amended with Zn, sediments were rolled twice weekly for 30 days (Simpson et al. 2004) and the pH was slightly adjusted with NaOH to raise the pH to within 0.3 pH units of the original sediments, ~7.3 (Hutchins et al. 2009).

Experimental design

Twelve flow-through artificial streams (flumes) were used to examine the effects of oxidized hyporheic flows on Zn exposure to *H. azteca* (Supplemental Data Figure S1). The flumes were constructed from 0.5-inch thick clear acrylic (Figure 2). Surface water and hyporheic water inputs were both sourced from Ann Arbor, MI municipal water after passing through activated carbon cartridges and a biofiltration tank. Water was delivered to two separate manifold systems with 12 water supply ports each (one for each flume). One manifold supplied surface water and the second manifold supplied hyporheic flows to each flume. Surface water flowed at 2.5 cm³/s and entered each flume through a holding tank on the upstream end of the flume. Water flowed over a spillover dam to provide surface water to the exposures in the main chamber of the flume without sediment disturbance. Hyporheic flows were set at 0.46 cm³/s (or 0.15 cm/min velocity), to simulate shallow, low residence time hyporheic flow. The flow rates were high enough to supply surface and hyporheic water continuously to the sediments, but low enough to prevent erosion or movement of sediments. The hyporheic flow rates were established primarily from the potential groundwater loading

velocities at the site the sediments were collected (2.0 m/d or 0.14 cm/min) (Baker et al. 2003). Other studies documented infiltration rates of 0.2 cm/min in sandy hyporheic sediments (i.e., < 2 mm) of headwater streams (Munn and Meyer 1988), and hyporheic sediments dominated by sand with intermediate hydraulic conductivity averaged 0.072 cm/min (Morrice et al. 1997). Both water sources flowed continuously during the experiments.

Each flume had one sediment exposure, either Zn-spiked (Zn) or reference (Ref), and two separate hyporheic exposures, hyporheic inputs (Hyp) and no hyporheic inputs (nonHyp). The four experimental treatments were: Zn-Hyp, Zn-nonHyp, Ref-Hyp and Ref-nonHyp. Six flumes contained reference sediments and six flumes contained Zn-spiked sediments. In each flume, two sediment baskets (200 cm² surface area, 8.3 cm deep) with open sides were used as the amphipod exposure units. Each basket was lined with mesh, filled with exposure sediments and placed in the artificial streams with sand as a filler substrate (Figure 2). Within each flume (Ref or Zn sediment), there were two baskets with the same sediment and different hyporheic exposures for six replicates per experimental treatment. To prevent effects of hyporheic inputs into the shared surface water, the upstream sediment exposure basket was a non-hyporheic exposure and the downstream exposure basket had a hyporheic input. Hyporheic water was delivered to the flume through a long flat porous airstone buried at the bottom of the sediment exposure basket on the downstream basket in each flume. Hyporheic water was pushed through the porous stone, into the overlying sediments and ultimately into the surface water.

Two 10-day experiments were performed on the same sediments with the same hyporheic conditions. An initial experiment (d0 to d10) took place before sediment aging under flow through conditions and a second aged experiment took place approximately

80 days later (d82 to d92). Aging of sediment under flow through conditions has shown to decrease toxicity of copper to *H. azteca* (Costello et al. 2015). Between experiments, sediments were continuously inundated with overlying water, which was renewed twice each week, but surface water did not flow continuously. Hyporheic flow was not present between experiments.

Chemistry sampling

Porewater sampling ports located laterally along each flume allowed for porewater sampling at 1.5-cm depth throughout the experiment (Figure 2). Porewater was extracted via rhizon samplers (0.19 μm filters). During the initial experiment, porewater was sampled on days 0, 1, 3, 5, 7 and 10. In the aged experiment, porewater was sampled on days 0, 2, 5 and 9 (or in total days: 82, 84, 87 and 91). From rhizon port-1 an 11-ml porewater sample was extracted and measured for dissolved oxygen (DO) (YSI Professional Plus ODO), pH (Thermo Scientific Orion Star A121) and temperature within ten minutes of sample collection. Prior to water quality measurements, 1-ml was extracted to measure reduced iron (Fe^{2+}), a redox indicator, using the Ferrozine method (Stookey 1970; Kostka and Luther 1994). Fe^{2+} is assumed to be inversely related to DO. Absorbance was measured on a spectrometer (Thermo Scientific Genesys 10uv scanning) the same day. From rhizon port-2, 10-ml of porewater was extracted and acidified with nitric acid to 2% for analysis of dissolved metals (Zn, Fe, and Mn) on an ICP-OES. On each sampling day, one surface water sample per flume was collected using a syringe, filtered on a 0.45 μm Millipore syringe-attached filter and acidified to 2% HNO_3^- for dissolved metal analysis on an ICP-OES. Blanks (MilliQ) were collected and acidified on each sampling day and sample metal concentrations were corrected for blank values.

ICP-OES detection limits were 50 $\mu\text{g/L}$ for Fe, 25 $\mu\text{g/L}$ for Mn, and 10 $\mu\text{g/L}$ for Zn. Six replicate porewater samples were collected each sampling day for all four treatment types.

Sediments were sampled at the beginning and end of both experiments. In the initial experiment, samples of both sediment types were frozen and stored upon sediment deployment, and then sediment cores were taken from each flume-basket on day 10. In the aged experiments, sediment cores were taken from each flume-basket on day 81 and day 92. For each experiment, 24 cores were extracted with six replicates for each of the four treatments. All sediment cores were taken using a 60-ml syringe (sawed to create a coring tube), then stored in a 50-ml centrifuge tube, the headspace purged with N_2 gas and stored frozen. Sediment samples were later thawed for acid volatile sulfide (AVS) and simultaneously extracted metals (SEM) analysis (Allen et al. 1991) (4 replicates per treatment), iron oxide content (total, amorphous and crystalline) (only 3 replicates per treatment) (Kostka and Luther 1994), dried for total metals (Zn, Fe, Mn) and combusted for organic carbon via loss-on-ignition (6 hour combustion at 450°C). For the total metal digestion, 0.5-g of dried sediment was digested in 7-ml of trace metal grade HNO_3 in a Hot Block (Environmental Express) at 112°C for 100 minutes according to method 3050B (US EPA 1996), then diluted 50 times for analysis on ICP-OES. During the digestion, metal concentrations were corrected for the sample analysis process using a procedural blank (MilliQ). Metal recovery from the digestion was verified ($>80\%$) by including standard reference sediment in the digestion. Iron oxide content was measured on ICP-MS.

Biological sampling

In both experiments, 7-14 day old *H. azteca* were exposed to sediment and hyporheic conditions in each flume-basket. Ten *H. azteca* were placed into a small plastic exposure chamber with 250- μm mesh on one side, to allow for surface water and sediment exposure to organisms (Costello et al. 2015). Endpoints for *H. azteca* included survival and growth.

Statistical analyses

Data analysis was performed in RStudio Version 1.1.453 (RStudio Team 2016). Linear mixed-effects models using packages lme4 (Bates et al. 2015) and lmerTest (Kuznetsova et al. 2017) assessed effects of both factors (Zn-amendment and hyporheic flow presence) over time on porewater chemistry. Main effects included sediment (Zn-spiked vs. reference), hyporheic flow (hyporheic vs. non-hyporheic) and time (as a continuous variable), with flume as a random effect. All two-way interactions between the three main effects were included in the models. Two-way interactions between sediment type and hyporheic flow tested for variation in porewater chemistry between the two sediments (Zn and Ref) caused by the hyporheic treatment. Two-way interactions between time and hyporheic flow tested for variation in porewater chemistry between the two hyporheic exposures over time. Two-way interactions between time and sediment tested for differences in porewater chemistry between sediment types over time. Main effects were only assessed in the results when factors were not involved in interactions with one another, though main effects are reported. Porewater variables with right skewed distributions were log-transformed for model analysis (porewater Fe^{2+} , Fe, Mn and Zn in the initial experiment and porewater Mn and Zn in the aged experiment).

Sediment chemistry endpoints with only one sampling time point (total metals, SEM-AVS, OC, Fe/Mn oxides) were assessed using linear mixed-effects models. Main effects in the model included hyporheic flow and Zn-spiked sediment, with flume as the random effect. Interactions tested for variation in sediment chemistry between the two sediments caused by hyporheic flows.

Effects of hyporheic flow and Zn-spiked sediment treatments on *H. azteca* survival were analyzed using generalized linear mixed-effects models (with binomial distribution) with flume as a random effect. Post-hoc tests of treatment-level differences were conducted using the multcomp package with a holm correction for multiple comparisons (Hothorn et al. 2008). Correlation analyses assessed relationships between continuous porewater and sediment chemistry parameters with biological parameters.

RESULTS

Initial sediment experiment

Porewater DO increased slightly in non-hyporheic exposures over time, but no changes in hyporheic exposures were observed over the ten days ($p = 0.043$) (Table 2). Non-hyporheic exposures had lower overall DO than hyporheic exposures and increased 27.8% over the 10 days, from 3.09 ± 0.24 mg/L (mean \pm SE) on day 1 to 3.94 ± 0.22 mg/L on day 10. Hyporheic exposures only increased by 4.3%, ranging from 4.46 ± 0.21 mg/L on day 1 to 4.65 ± 0.18 mg/L on day 10 (Figure 3A). There was no effect of sediment treatment on DO ($p = 0.97$).

Overall, Fe^{2+} was higher in the non-hyporheic exposures compared to the hyporheic exposures ($p < 0.001$) (Table 2), as expected from DO concentrations. In both

hyporheic exposures, Fe^{2+} remained near 0.00 mg/L throughout most of the experiment, indicating near complete oxidation caused by the hyporheic treatment. On day 10, Fe^{2+} in the Ref-Hyp exposure was 98.9% lower than in Ref-nonHyp (0.15 ± 0.13 mg/L and 13.29 ± 1.97 mg/L, respectively), and the Zn-Hyp exposure had Fe^{2+} concentrations that were 90.7% lower than Zn-nonHyp (0.28 ± 0.25 mg/L and 2.96 ± 0.48 mg/L, respectively) (Figure 3B). Fe^{2+} in the zinc-spiked sediment treatments increased more over the 10 days, compared to Ref sediments ($p = 0.019$) (Table 2). The Zn-spiked sediments increased 41.8% from 1.14 ± 0.42 mg/L on day 1 to 1.62 ± 0.48 mg/L on day 10. The Ref sediment Fe^{2+} concentrations increased 36.6%, from 4.92 ± 1.44 mg/L on day 1 to 6.72 ± 2.19 mg/L on day 10.

Porewater pH varied more between the hyporheic exposures of the Zn-spiked sediments, compared to the Ref sediments ($p < 0.001$) (Table 2, Figure 3C). The pH was on average higher in the Zn-Hyp exposure than in Zn-nonHyp (7.58 ± 0.05 and 7.29 ± 0.04 , respectively), whereas Ref-Hyp was more similar to Ref-nonHyp (7.48 ± 0.03 and 7.42 ± 0.03 , respectively). The Zn-spiked sediments exhibited greater increase in pH over time, compared to the Ref sediments ($p = 0.002$) (Table 2). The pH in the Zn-spiked exposures increased from 7.04 ± 0.04 on day 0 to 7.60 ± 0.04 for Zn-nonHyp and to 7.92 ± 0.07 for Zn-Hyp on day 10 (Figure 3C). The reference sediment pH increased less over time, ranging from a pH of 7.31 ± 0.07 on day 0 to 7.67 ± 0.02 in Ref-nonHyp and to 7.78 ± 0.04 Ref-Hyp on day 10. The pH increase over time was likely related to porewater pH equilibration with the surface waters, which had an average pH of $8.12 \pm$

0.06. The pH in these systems was generally buffered against the release of dissolved metals (Zn^{2+}), as the alkalinity of input water was moderate ($\sim 55 \text{ mg/L CaCO}_3$).

A significant interaction between hyporheic flow and sediment ($p = 0.002$) is illustrated by the greater difference in porewater Fe between non-hyporheic and hyporheic exposures in the Ref sediments ($8.29 \pm 0.50 \text{ mg/L}$ in Ref-nonHyp vs. $1.42 \pm 0.42 \text{ mg/L}$ in Ref-Hyp) compared to the Zn-spiked sediments ($1.54 \pm 0.14 \text{ mg/L}$ in Zn-nonHyp vs. $0.32 \pm 0.09 \text{ mg/L}$ in Zn-Hyp). The effect of the hyporheic treatment was greater in Ref than in Zn sediments, likely because porewater Fe was initially higher in the Ref ($6.04 \text{ mg/L} \pm 0.87 \text{ SE}$) than in the Zn-spiked sediments ($1.03 \text{ mg/L} \pm 0.22 \text{ SE}$). Porewater Fe decreased in the hyporheic exposures over time, whereas in the non-hyporheic exposures, porewater Fe increased slightly ($p = 0.003$) (Figure 4A). In Ref-Hyp porewater Fe declined by 95.6% ($6.09 \pm 1.12 \text{ mg/L}$ to $0.26 \pm 0.11 \text{ mg/L}$) and in Zn-Hyp by 84.3% ($1.14 \pm 0.38 \text{ mg/L}$ to $0.18 \pm 0.03 \text{ mg/L}$). Whereas in the non-hyporheic exposures, porewater Fe increased over time, by 50.5% in Ref-nonHyp ($5.99 \pm 1.45 \text{ mg/L}$ to $9.02 \pm 1.37 \text{ mg/L}$) and by 82.2% in Zn-nonHyp ($0.92 \pm 0.27 \text{ mg/L}$ to $1.68 \pm 0.24 \text{ mg/L}$). At the end of the experiment on day 10, porewater Fe was correlated positively with Fe^{2+} ($r = 0.97$, $p < 0.001$) and negatively with DO ($r = -0.52$, $p = 0.008$), indicating decreases in porewater Fe with sediment oxidation.

Porewater Mn concentrations were lower in the hyporheic exposures, relative to the non-hyporheic exposures ($p = 0.024$) (Table 2). Porewater Mn was 74.9% lower in the Ref-Hyp ($190.3 \pm 56.7 \text{ } \mu\text{g/L}$) than in Ref-nonHyp ($759.3 \pm 45.2 \text{ } \mu\text{g/L}$), while in the Zn-spiked sediments, porewater Mn was 63.1% lower in Zn-Hyp ($452.5 \pm 120.0 \text{ } \mu\text{g/L}$)

than in Zn-nonHyp ($1225.9 \pm 92.6 \mu\text{g/L}$). Hyporheic exposures experienced a greater decline in porewater Mn over time, compared to non-hyporheic exposures ($p = 0.001$) (Figure 4B). On day 0 of the experiment, porewater Mn concentrations were their highest, $1855.5 \pm 161.4 \mu\text{g/L}$ in the Zn-spiked sediments and $911.3 \pm 70.8 \mu\text{g/L}$ in the Ref sediments. By day 10, the non-hyporheic exposures experienced moderate declines in porewater Mn, Zn-nonHyp decreased 55.6% to $823.1 \pm 87.2 \mu\text{g/L}$ and Ref-nonHyp declined 31.0% to $629.1 \pm 92.3 \mu\text{g/L}$. The hyporheic exposures had a greater percent decrease, the Zn-Hyp decreased 95.4% to $84.6 \pm 35.8 \mu\text{g/L}$ and Ref-Hyp decreased 97.7% to $20.7 \pm 4.0 \mu\text{g/L}$. On day 10, porewater Mn concentrations correlated positively with Fe^{2+} ($r = 0.56$, $p = 0.004$) and negatively with pH ($r = -0.67$, $p < 0.001$).

Porewater Zn was affected by hyporheic exposure, sediment type and time. There was a larger magnitude of difference in porewater Zn between hyporheic and non-hyporheic exposures in the Zn-spiked sediments, compared to the Ref sediments ($p < 0.001$) (Table 2, Figure 4C). Porewater Zn decreased over time in the Zn-spiked exposures only, not in the Ref ($p < 0.001$) (Figure 4C). Day 0 porewater Zn concentrations averaged $2299.9 \pm 228.2 \mu\text{g/L}$ in the Zn sediments and $12.2 \pm 5.1 \mu\text{g/L}$ in the Ref sediments. By day 10, the porewater Zn in the Zn-nonHyp exposure declined by 62.6% ($859.4 \pm 91.5 \mu\text{g/L}$) and the Zn-Hyp exposure declined by 85.9% ($324.6 \pm 54.1 \mu\text{g/L}$). Porewater Zn correlated with porewater Mn ($r = 0.56$, $p = 0.005$), and their trends overtime were similar (Figure 4A, 4C).

Total metals were affected by both sediment and hyporheic flows. There was no effect of hyporheic flow on total Fe ($p = 0.406$), but total Fe was higher in the Ref

sediments (5.28 ± 0.27 g/kg) than in the Zn-spiked (4.21 ± 0.12 g/kg) ($p = 0.006$) (Table 2). Total Mn was lower in the Zn-spiked sediments than the Ref sediments ($p = 0.013$) and there was no significant hyporheic effect (at $\alpha = 0.05$). Total Zn was lower in the Zn-Hyp exposure (378.7 ± 17.5 mg/kg) compared to the Zn-nonHyp exposure (420.7 ± 11.8 mg/kg) ($p = 0.035$), and no differences were observed between the Ref exposures. This could be due to a possible loss of total Zn from the system with hyporheic inputs.

Metal binding ligands were also affected by the hyporheic treatment. Hyporheic exposures had lower AVS than non-hyporheic exposures ($p = 0.027$), but there was no difference in AVS between Ref and Zn-spiked sediments ($p = 0.918$). This indicates that regardless of sediment type, AVS was lower in the hyporheic exposures. Despite differences in AVS between the hyporheic treatments, there was no effect of hyporheic treatment on $(Zn_{SEM}-AVS)/fOC$ ($p = 0.818$), but the Zn-spiked sediments had higher overall $(Zn_{SEM}-AVS)/fOC$ than the Reference sediments ($p < 0.001$) (Figure 5A).

Amorphous Fe oxide was higher in Ref sediments than Zn-spiked ($p = 0.001$), but there were no differences between hyporheic exposures ($p = 0.399$) (Supplemental Data Table S1). Total oxidized Fe was higher in the non-hyporheic exposure compared to the hyporheic exposure ($p = 0.037$), but not affected by sediment ($p = 0.253$). Amorphous Mn oxide was unaffected by both treatments, but total and crystalline Mn oxides were both greater in Ref sediments than Zn-spiked sediment ($p = 0.023$, $p = 0.032$, respectively). Mn oxides were not affected by hyporheic flow. Zn bound to amorphous, total and crystalline Fe/Mn oxides was higher in the Zn-spiked sediments than reference sediments ($p < 0.001$, $p < 0.001$, $p = 0.079$) and not affected by hyporheic flow.

The survival of *H. azteca* declined in response to both hyporheic exposure ($p < 0.001$) and Zn-spiked sediment ($p = 0.003$) (Figure 6A). The proportion of *H. azteca* survival was highest in the Ref-nonHyp exposures (0.82 ± 0.11) and lowest in the Zn-Hyp exposure (0.00 ± 0.00). In multiple comparison tests, there was no difference in survival between the Ref-Hyp (0.37 ± 0.16) and Zn-nonHyp (0.43 ± 0.11) ($p = 0.648$), but both had lower survival than Ref-nonHyp and higher survival than Zn-Hyp. The unexpected low survival in the Ref-Hyp exposure, compared to the Ref-nonHyp exposure, was likely due to the visible Fe oxidation on the Ref-Hyp sediments during the 10-day exposure. A thick mat of Fe flocculent developed on the sediment surface in the Ref-Hyp exposure (Supplemental Data Figure S2). The iron oxidation did not occur in either non-hyporheic exposure or in the Zn hyporheic exposure, possibly a product of the sediment spiking procedure and inhibition of iron oxidizing microbial communities.

Aged sediment experiment

Porewater redox conditions were more stable over time during the aged sediment experiment. The hyporheic exposures continued to have higher DO than the non-hyporheic exposures, and this relationship was greater for Ref than Zn-spiked sediments ($p = 0.003$) (Table 3). DO in Ref-Hyp (4.87 ± 0.15 mg/L) was 105% higher than Ref-nonHyp (2.37 ± 0.05 mg/L), whereas in Zn-spiked sediments, DO in Zn-Hyp (4.47 ± 0.22 mg/L) was only 69% higher than Zn-nonHyp (2.65 ± 0.05 mg/L) (Figure 3D). DO did not change over time ($p = 0.47$). Fe^{2+} was also no longer affected by time ($p = 0.14$). The lower Fe^{2+} resulting from hyporheic flows was disproportionately larger in the Ref sediments compared to Zn-spiked sediments ($p < 0.001$) (Table 3, Figure 3E). Ref-Hyp

(0.04 ± 0.01 mg/L) was 99.5% lower than Ref-nonHyp (8.62 ± 0.60 mg/L), whereas Zn-Hyp (1.43 ± 0.40 mg/L) was 75.2% lower than Zn-nonHyp (5.78 ± 0.28 mg/L).

Porewater pH returned to the original pH of sediments before the initial experiment, ~ 7.3 (Figure 3F). Porewater pH was relatively higher in the Ref-nonHyp exposure (7.24 ± 0.04) compared to the Ref-Hyp exposure (7.13 ± 0.05), whereas there was little difference in pH between Zn-nonHyp (7.13 ± 0.03) and Zn-Hyp (7.17 ± 0.04) exposures ($p = 0.004$) (Table 3). Surface water pH remained high throughout the experiment at ~ 7.7 to 7.8 in each flume.

The difference between hyporheic exposures on porewater Fe was greater in the Ref sediments than the Zn-spiked sediments ($p < 0.001$) (Figure 4D). Porewater Fe was on average 98% lower in Ref-Hyp (0.12 ± 0.03 mg/L) compared to Ref-nonHyp (6.44 ± 0.31 mg/L), whereas in the Zn-spiked sediments, Zn-Hyp (0.94 ± 0.26 mg/L) was 80% lower than Zn-nonHyp (4.80 ± 0.38 mg/L). Porewater Fe also decreased slightly over time across all treatments ($p = 0.034$)

The difference in porewater Mn was relatively higher between the Zn-spiked exposures compared to the Ref exposures ($p = 0.001$) (Table 3, Figure 4E). Porewater Mn was 96.0% lower on average in Zn-Hyp (28.5 ± 6.5 $\mu\text{g/L}$) compared to Zn-nonHyp (717.0 ± 77.5 $\mu\text{g/L}$), whereas in Ref sediments porewater Mn was 80.4% lower in Ref-Hyp (9.2 ± 2.6 $\mu\text{g/L}$) than in Ref-nonHyp (418.1 ± 25.8 $\mu\text{g/L}$). Despite the higher Mn concentrations in the non-hyporheic exposures compared to the hyporheic exposures, porewater Mn in the hyporheic exposures decreased more over time than the non-hyporheic exposures ($p = 0.002$). This relationship was largely driven by the reference

sediments; porewater Mn decreased 79.7% in Ref-Hyp compared to 23.7% in Ref-nonHyp, whereas Zn-Hyp decreased 27.0% and Zn-nonHyp declined 19.2% (Figure 4E).

There was no effect of hyporheic flows on porewater Zn in the aged experiment, but the Zn-spiked sediments still maintained higher porewater Zn than Ref sediments ($p < 0.001$) (Table 3, Figure 4F). Porewater Zn concentrations averaged $146.3 \pm 10.8 \mu\text{g/L}$ in the Zn-spiked sediments and were generally at or below detection limits in the Ref sediments ($< 5.0 \mu\text{g/L}$).

While total metals were unaffected by hyporheic flows (Table 3), redox sensitive binding ligands were affected by the hyporheic exposure. The interaction between hyporheic flow and sediment type on $(\text{Zn}_{\text{SEM}}\text{-AVS})/f\text{OC}$ indicates greater potential Zn bioavailability in the Zn-Hyp exposure compared to Zn-non-Hyp ($p = 0.001$) (Table 3). Zn-Hyp exposure had 39.7% more bioavailable Zn (i.e., $(\text{Zn}_{\text{SEM}}\text{-AVS})/f\text{OC}$) than Zn-nonHyp (Table 1; Figure 5B). This relationship is a product of slightly higher Zn_{SEM} and lower $f\text{OC}$ in the Zn-Hyp exposure, compared to Zn-nonHyp (Table 3). Zn_{SEM} was also influenced by an interaction between sediment and hyporheic flows ($p = 0.014$). AVS was higher the non-hyporheic sediments than the hyporheic sediments ($p = 0.028$), driven largely by the lower AVS in Ref-Hyp compared to the other exposures ($p = 0.024$).

Amorphous Fe oxides remained higher in Ref than Zn-spiked sediments ($p < 0.001$), but no effects of treatment were found in total or crystalline Fe oxides (Supplemental Data Table S1). Amorphous Mn oxides were higher in non-hyporheic exposures, compared to hyporheic ($p = 0.014$), and higher in Ref than Zn-spiked sediments ($p = 0.035$). Multiple comparison tests revealed that this relationship was

largely drive by the Zn-Hyp exposure, which had lower amorphous Mn oxide than Zn-nonHyp ($p < 0.001$), Ref-Hyp ($p = 0.048$) and Ref-nonHyp ($p < 0.001$) exposures. Zn bound to amorphous, total and crystalline Fe/Mn oxides was greater in Zn-spiked than Ref sediments for all three models ($p < 0.001$, $p < 0.001$, $p = 0.003$), but was consistently unaffected by hyporheic flow.

Despite no differences in porewater Zn or total Zn in the hyporheic exposures, there was still an effect of hyporheic flows on *H. azteca* survival on day 10. There was a significant interaction between Zn-spiked sediment and hyporheic flows ($p = 0.019$). Though there was no difference in survival between the Ref sediments (0.88 ± 0.03 in Ref-nonHyp and 0.90 ± 0.05 in Ref-Hyp), survival in the Zn-Hyp exposure was lower (0.10 ± 0.04) than the in Zn-nonHyp exposure (0.43 ± 0.11) (Figure 5B). Throughout the 10-day aged experiment, sediment Zn concentrations (406 ± 19 mg/kg) were lower than the sediment PEC for Zn (459 mg/kg) and porewater Zn concentrations (146 ± 11 μ g/L) were just above the PEC for Zn in freshwaters (120 μ g/L).

Comparison of initial and aged experiments

Porewater chemistry was more stable during the aged experiment compared to the initial experiment. The pH stabilized to the original pH of the sediments (~ 7.30), before sediment and hydrologic (surface and hyporheic flow) manipulations, and porewater DO, Fe^{2+} and pH were constant throughout the 10-day aged experiment. Porewater Zn was also stable over time in the aged experiment, though porewater Fe and Mn still decreased slightly over time. Porewater Zn in the aged experiment was the same for the Zn-Hyp and Zn-nonHyp exposures, indicating that, despite the differences in redox chemistry (Fe^{2+} ,

pH) and binding capacity (i.e., $(Zn_{SEM-AVS})/fOC$) there was no longer an effect of hyporheic treatment on porewater Zn.

Survival of *H. azteca* varied between experiments. In the initial experiment, *H. azteca* survival declined in response to hyporheic flow induced Fe-oxidation in the Ref sediments, and survival was more negatively correlated with Fe^{2+} ($r = -0.62$, $p = 0.001$), as opposed to other porewater or sediment parameters like $(Zn_{SEM-AVS})/fOC$ ($r = -0.53$, $p = 0.007$). Whereas in the aged experiment, there was no visible Fe-oxidation in the Ref-Hyp exposure, and survival was high. In the aged experiment, *H. azteca* survival was more correlated with total Zn ($r = -0.86$, $p < 0.001$), $(Zn_{SEM-AVS})/fOC$ ($r = -0.84$, $p < 0.001$) and porewater Zn ($r = -0.59$, $p = 0.003$). Despite similar porewater Zn concentrations in Zn-Hyp and Zn-nonHyp exposures in the aged experiment, there was still decreased survival associated with the Zn-Hyp exposure, relative to Zn-nonHyp exposure. This difference was not related to porewater Zn or total Zn, but may be related to $(Zn_{SEM-AVS})/fOC$, as it was higher in Zn-Hyp than Zn-nonHyp in the aged experiment (Figure 5B).

DISCUSSION

Hyporheic flow and ecological risk

This study established the important role of hyporheic flows on sediment redox chemistry and metal bioavailability. As hypothesized, the zinc-contaminated sediments with hyporheic exposure (Zn-Hyp) were more oxidized than the zinc-contaminated sediments without hyporheic flow (Zn-nonHyp) and they released more zinc from the sediments. This resulted in greater exposure and effects on *H. azteca* in the hyporheic

compared to non-hyporheic zinc-contaminated sediments. Though we expected to see *H. azteca* survival increase over time from the initial to the aged experiment, there was little difference in survival between experiments.

These relationships are particularly critical for streams, where downwelling zones in riffles are characterized by oxidized hyporheic sediments (Hendricks and White 1991; Franken et al. 2001), as simulated in our study. Downwelling zones are typically located at the upstream end of riffles in streams and have greater benthic macroinvertebrate community diversity and sensitivity, compared to the downstream ends of riffles (Davy-Bowker et al. 2006), which are characterized by more reduced hyporheic conditions (Boulton 1993). Based on *H. azteca* responses in this study, more sensitive benthic macroinvertebrate communities residing in downwelling zones could be at higher risk in metal contaminated streams, compared to benthic communities in upwelling zones, pools or other stream habitat with limited groundwater-surface water interaction.

H. azteca responses also showed how metal bioavailability in sediments changes through time in relation to hyporheic flows. Survival in the Zn-spiked treatments of the initial experiment was associated with greater porewater Zn release from Zn-Hyp exposure compared to Zn-nonHyp. While the initial experiment was not yet in equilibrium (due to changing pH, D.O, Fe²⁺ and dissolved metals over the ten days), the aged experiment was in equilibrium, as there were few changes in porewater chemistry over the ten day experiment. Despite the lack of difference in porewater Zn or total Zn concentrations between Zn-Hyp and Zn-nonHyp exposures in the aged experiment, *H. azteca* survival was lower in the Zn-Hyp exposure compared to Zn-nonHyp. This may be linked to $(Zn_{SEM}-AVS)/fOC$, which was higher in the Zn-Hyp exposure than the Zn-

nonHyp in the aged experiment only, and well above toxic thresholds ($\sim 150 \mu\text{mol/g}$) for $(\text{Zn}_{\text{SEM}}\text{-AVS})/f\text{OC}$ (Burton et al. 2005). The elevated bioavailable Zn likely resulted from the low AVS and $f\text{OC}$ content in the sediments. In addition, there may have been dietary exposure from the epibenthic feeding. This suggests the potential for long-term effects to biota if SEM is elevated with respect to AVS and organic carbon in downwelling zones.

Though total Fe and Mn were relatively high in these sediments, there were no effects of hyporheic flow on Zn bound to Fe/Mn oxide minerals. In the aged experiment, amorphous Mn oxide was lower in the Zn-Hyp exposure than in Zn-nonHyp and both reference treatments. This suggests a lower capacity in the sediments for Zn to bind to amorphous Mn oxide in the Zn-Hyp exposure, which could potentially contribute to higher *H. azteca* toxicity, though Zn bound to amorphous Fe/Mn oxides was not statistically influenced by hyporheic flow. Formation of Mn oxides in the hyporheic zone is influenced by porewater residence times (Harvey and Fuller 1998), which may have been too short in this experiment for Mn oxide formation. The effect of hyporheic flow on total oxidized Fe during the initial experiment was likely related to loss of oxidized Fe from the Ref-Hyp exposure during floc formation. In oxidized environments, Fe/Mn oxide minerals are important for metal binding (Danner et al. 2015) and may increase binding within the hyporheic zone specifically (Fuller and Harvey 2000). Future investigations into the role of Fe/Mn oxides as metal binding ligands in the hyporheic zone are warranted.

Toxicity of the Ref-Hyp exposure during the initial experiment was unexpected, but the significant formation of flocculent mats on the sediment surface suggests that excess iron oxidation decreased survival. This floc formation was similar to iron

oxidization of groundwater in streams. It is possible the flocculent caused physical toxicity to *H. azteca* (Vuori 1995). Toxicity could result from excess ingestion as well, as mayflies have been observed physically removing iron precipitates (Gerhardt 1992). The flocculation effect was also limited to the hyporheic exposure in the Ref sediments of the initial experiment, indicating this was a hyporheic-induced effect. The ZnCl_2 spike and subsequent lower pH may have impaired or decreased the Fe-oxidizing microbial communities in Zn-spiked sediments, which was why the Fe flocculent only formed on Ref sediments and not Zn-spiked sediments. In soils, ZnCl_2 spiking caused complete inhibition of nitrogen fixing bacteria at 0.5 mg/L Zn Cl_2 (Cela and Sumner 2002). Porewater Zn concentrations were at 2.0 mg/L at the beginning of this study, suggesting that sediment spiking may be responsible for the lack of Fe oxidation in the Zn-Hyp exposure.

Implications for risk assessment

These findings demonstrate the important role of hyporheic flows on sediment redox chemistry and metal bioavailability. The laboratory experiments provided an assessment of mechanistic effects of zinc contaminated sediments and oxic hyporheic flows. While other studies have examined the important differences in redox chemistry resulting from hyporheic flows (Hendricks et al. 1993); our study linked hyporheic flow processes with metal fate and biotic effects, and may have important implications for ecological risk assessments in aquatic ecosystems.

Monitoring of hyporheic conditions in metal contaminated ecosystems is critical to determine if the hyporheic zone is an important contaminant exposure route, and to

understand metal speciation and bioavailability. The USEPA has recommended these processes be considered in ecological risk assessment and provided guidance on their incorporation in risk assessment (U.S. EPA 2008). Hyporheic flow inputs can be measured in the field with the installation of relatively simple equipment.

Minipiezometers provide an inexpensive and simple way to measure upwelling and downwelling in shallow sediments via changes in hydraulic head (Winter 1999; Baxter et al. 2003; Rivett et al. 2008). Hyporheic flow direction and magnitude can also be estimated by measuring differences in streambed temperature and depth in the field using a variety of temperature loggers (Hatch et al. 2006; Keery et al. 2007; Gordon et al. 2012). Comparisons of porewater chemistry and contaminant concentrations could then be made among sites with upwelling, downwelling and those without hyporheic flow.

As observed in the field study of groundwater-surface water interactions with chlorobenzene toxicity and bioaccumulation (Greenberg et al. 2002), it is important to document hyporheic-related contamination in order to link exposures with effects (U.S. EPA 2008). This research demonstrates the importance of hyporheic flows on redox-sensitive binding ligands and the subsequent effects on aquatic biological communities. Inclusion of hyporheic flows in ecological risk assessments could more accurately characterize metal exposure pathways to stream aquatic biota.

REFERENCES

Allen HE, Fu G, Boothman WS, DiToro DM, Mahony JD. 1991. Determination of acid volatile sulfide and selected simultaneously extractable metals in sediment. EPA 821/R-91/100.

Baker ME, Wiley MJ, Seelbach PW. 2003. GIS-based models of potential groundwater loading in glaciated landscapes : considerations and development in Lower Michigan. *Fish Res.*(2064).

Bates D, Maechler M, Bolker B, Walker S. 2015. Linear Mixed-Effects Models Using lme4. *J Stat Softw.* 67(1):1–48. doi:10.18637/jss.v067.i01.

Baxter C, Hauer FR, Woessner WW. 2003. Measuring groundwater – stream water exchange: New techniques for installing minipiezometers and estimating hydraulic conductivity. *Trans Am Fish Soc.* 132:493–502. doi:10.1577/1548-8659(2003)132<0493:MGWENT>2.0.CO;2.

Boulton AJ. 1993. Stream ecology and surface-hyporheic hydrologic exchange: Implications, techniques and limitations. *Aust J Mar Freshw Res.* 44:553–564. doi:10.1071/MF9930553.

Brunke M, Gonser T. 1997. The ecological significance of exchange processes between rivers and groundwater. *Freshw Biol.* 37:1–33. doi:10.1046/j.1365-2427.1997.00143.x.

Burton GA, Nguyen LTH, Janssen C, Baudo R, McWilliam R, Bossuyt B, Beltrami M, Green A. 2005. Field validation of sediment zinc toxicity. *Environ Toxicol Chem.* 24(3):541–553. doi:10.1897/04-031R.1.

Calmano W, Hong J, Forstner U. 1993. Binding and mobilization of heavy metals in contaminated sediments affected by pH and redox potential. *Water Sci Technol Tech.* 28:223–235. doi:10.2166/wst.1993.0622.

Cela S, Sumner ME. 2002. Soil zinc fractions determine inhibition of nitrification. *Water Air Soil Pollut.* 141:91–104. doi:10.1023/A:1021379421878.

Chapman PM, Wang F, Janssen C, Persoone G, Allen HE. 1998. Ecotoxicology of metals in aquatic sediments: binding and release, bioavailability, risk assessment, and remediation. *Can J Fish Aquat Sci.* 55(10):2221–2243. doi:10.1139/f98-145.

Cooper MJ, Rediske RR, Uzarski DG, Burton TM. 2001. Sediment contamination and faunal communities in two subwatersheds of Mona Lake, Michigan. *J Environ Qual.* 38:1255–1265. doi:10.2134/jeq.2008.0429.

Costello DM, Hammerschmidt CR, Burton GA. 2015. Copper Sediment Toxicity and Partitioning during Oxidation in a Flow-Through Flume. *Environ Sci Technol.* 49(11):6926–6933. doi:10.1021/acs.est.5b00147.

Danner KM, Hammerschmidt CR, Costello DM, Burton GA. 2015. Copper and nickel partitioning with nanoscale goethite under variable aquatic conditions. *Environ Toxicol Chem.* 34(8):1705–1710. doi:10.1002/etc.2977.

Davy-Bowker J, Sweeting W, Wright N, Clarke RT, Arnott S. 2006. The distribution of benthic and hyporheic macroinvertebrates from the heads and tails of riffles. *Hydrobiologia.* 563(1):109–123. doi:10.1007/s10750-005-1482-9.

Feris K, Ramsey P, Frazar C, Moore JN, Gannon JE, Holben WE. 2003. Differences in hyporheic-zone microbial community structure along a heavy-metal contamination gradient. *Appl Environ Microbiol.* 69(9):5563–5573. doi:10.1128/AEM.69.9.5563.

Feris KP, Ramsey PW, Gibbons SM, Frazar C, Rillig MC, Moore JN, Gannon JE, Holben WE. 2009. Hyporheic microbial community development is a sensitive indicator of metal contamination. *Environ Sci Technol.* 43(16):6158–6163.

doi:10.1021/es9005465.

Franken RJM, Storey RG, Williams DD. 2001. Biological, chemical and physical characteristics of downwelling and upwelling zones in the hyporheic zone of a north-temperature stream. *Hydrobiologia.* 444:183–195. doi:10.1023/A:1017598005228.

Fuller CC, Harvey JW. 2000. Reactive uptake of trace metals in the hyporheic zone of a mining-contaminated stream, Pinal Creek, Arizona. 34(7):1150–1155.

doi:10.1021/es990714d.

Gerhardt A. 1992. Effects of subacute doses of iron (Fe) on *Leptophlebia marginata* (Insecta: Ephemeroptera). *Freshw Biol.* 27(1):79–84. doi:10.1111/j.1365-

2427.1992.tb00524.x.

Gibert J, Plénet S, Marmonier P, Vanek V. 1995. Hydrological exchange and sediment characteristics in a riverbank: relationship between heavy metals and invertebrate community structure. *Can J Fish Aquat Sci.* 52(1974):2084–2097. doi:10.1139/f95-202.

Gordon RP, Lautz LK, Briggs M a., McKenzie JM. 2012. Automated calculation of vertical pore-water flux from field temperature time series using the VFLUX method and computer program. *J Hydrol.* 420–421:142–158. doi:10.1016/j.jhydrol.2011.11.053.

Greenberg MS, Burton GA, Rowland CD. 2002. Optimizing interpretation of in situ effects of riverine pollutants: impact of upwelling and downwelling. *Environ Toxicol*

Chem. 21(2):289–97. doi:10.1002/etc.5620210210.

Harvey JW, Fuller CC. 1998. Effect of enhanced manganese oxidation in the hyporheic zone on basin-scale geochemical mass balance. *Water Resour Res.* 34(4):623. doi:10.1029/97WR03606.

Hatch CE, Fisher AT, Revenaugh JS, Constantz J, Ruehl C. 2006. Quantifying surface water-groundwater interactions using time series analysis of streambed thermal records: Method development. *Water Resour Res.* 42(10). doi:10.1029/2005WR004787.

Hendricks SP, Journal S, American N, Society B, Mar N. 1993. Microbial ecology of the hyporheic zone: A perspective integrating hydrology and biology. *J North Am Benthol Soc.* 12(1):70–78. doi:10.2307/1467687.

Hendricks SP, White DS. 1991. Physicochemical patterns within a hyporheic zone of a Northern Michigan river, with comments on surface water patterns. *Can J Fish Aquat Sci.* 48(9):1645–1654. doi:10.1139/f91-195.

Hendricks SP, White DS. 2000. Stream and groundwater influences on phosphorous biogeochemistry. In: Jones JB, Mulholland PJ, editors. *Streams and Groundwaters*. San Diego, CA USA: Academic Press. p. 221–235.

Hothorn T, Bretz F, Westfall P. 2008. Simultaneous Inference in General Parametric Models. *Biometrical J.* 50(3):346–363. doi:10.1002/bimj.200810425.

Hutchins CM, Teasdale PR, Lee SY, Simpson SL. 2009. The effect of sediment type and pH-adjustment on the porewater chemistry of copper- and zinc-spiked sediments. *Soil*

Sediment Contam. 18:55–73. doi:10.1080/15320380802545407.

Keery J, Binley A, Crook N, Smith JWN. 2007. Temporal and spatial variability of groundwater-surface water fluxes: Development and application of an analytical method using temperature time series. *J Hydrol.* 336:1–16. doi:10.1016/j.jhydrol.2006.12.003.

Kostka JE, Luther GW. 1994. Partitioning and speciation of solid phase iron in saltmarsh sediments. *Geochim Cosmochim Acta.* 58(7):1701–1710. doi:10.1016/0016-7037(94)90531-2.

Kuznetsova A, Brockhoff PB, Christensen RHB. 2017. Package: Tests in Linear Mixed Effects Models. *J Stat Softw.* 82(13):1–26. doi:10.18637/jss.v082.i13.

MacDonald DD, Ingersoll CG, Berger TA. 2000. Development and evaluation of consensus-based sediment quality guidelines for freshwater ecosystems. *Arch Environ Contam Toxicol.* 39:20–31. doi:10.1007/s002440010075.

Mathers KL, Millett J, Robertson AL, Stubbington R, Wood PJ. 2014. Faunal response to benthic and hyporheic sedimentation varies with direction of vertical hydrological exchange. *Freshw Biol.* 59:2278–2289. doi:10.1111/fwb.12430.

Mendonca RM, Daley JM, Hudson ML, Schlekot C, Burton GA, Costello D. 2017. Metal oxides in surface sediment control nickel bioavailability to benthic macroinvertebrates. *Environ Sci Technol.* 51:13407–13416. doi:10.1021/acs.est.7b03718.

Moldovan OT, Levei E, Marin C, Banciu M, Banciu HL, Pavelescu C, Brad T, Cîmpean M, Meleg I, Iepure S, et al. 2011. Spatial distribution patterns of the hyporheic

invertebrate communities in a polluted river in Romania. *Hydrobiologia*. 669:63–82.
doi:10.1007/s10750-011-0651-2.

Morrice JA, Valett HM, Dahm CN, Campana ME. 1997. Alluvial characteristics, groundwater-surface water exchange and hydrological retention in headwater streams. *Hydrological Process*. 11(3):253–267. doi:10.1002/(SICI)1099-1085(19970315)11:3<253::AID-HYP439>3.0.CO;2-J.

Munn NL, Meyer JL. 1988. Rapid flow through the sediments of a headwater stream in the southern Appalachians. *Freshw Biol*. 20(2):235–240. doi:10.1111/j.1365-2427.1988.tb00447.x.

Nelson SM, Roline RA. 1999. Relationships between metals and hyporheic invertebrate community structure in a river recovering from metals contamination. *Hydrobiologia*. 397:211–226. doi:10.1023/A:1003734407788.

Olsen DA, Townsend CR. 2003. Hyporheic community composition in a gravel-bed stream: influence of vertical hydrological exchange, sediment structure and physicochemistry. *Freshw Biol*. 48:1363–1378. doi:10.1046/j.1365-2427.2003.01097.x.

Rehg KJ, Packman AI, Ren J. 2005. Effects of suspended sediment characteristics and bed sediment transport on streambed clogging. *Hydrological Process*. 19:413–427. doi:10.1002/hyp.5540.

Rivett MO, Ellis PA, Greswell RB, Ward RS, Roche RS, Cleverly MG, Walker C, Conran D, Fitzgerald PJ, Willcox T, et al. 2008. Cost-effective mini drive-point piezometers and multilevel samplers for monitoring the hyporheic zone. *Q J Eng Geol*

Hydrogeol. 41:49–60. doi:10.1144/1470-9236/07-012.

RStudio Team. 2016. RStudio: Integrated Development for R. RStudio, Inc., Boston, MA
URL <http://www.rstudio.com/>.

Simpson SL, Angel BM, Jolley DF. 2004. Metal equilibration in laboratory-contaminated (spiked) sediments used for the development of whole-sediment toxicity tests. *Chemosphere*. 54(5):597–609. doi:10.1016/j.chemosphere.2003.08.007.

Steinman A, Rediske R, Denning R, Nemeth L, Uzarski D, Biddanda B, Luttenton M. 2003. Preliminary watershed assessment: Mona Lake Watershed. Scientific Technical Reports. Paper 9.

Stookey LL. 1970. Ferrozine - a new spectrophotometric reagent for iron. *Anal Chem*. 42(7):779–781. doi:10.1021/ac60289a016.

U.S. EPA. 2008. Evaluating Ground-Water/Surface-Water Transition Zones in Ecological Risk Assessment. EPA-540-R06-072. Washington, D.C.

US EPA. 1996. Method 3050B - Acid digestion of sediments, sludges, and soils. Revision 2.

Vuori K-M. 1995. Direct and indirect effects of iron on river ecosystems. *Ann Zool Fennici*. 32(3):317–329. doi:0003-445X.

Winter TC. 1999. Relation of streams , lakes , and wetlands to groundwater flow systems. *Hydrogeol J*. 7:28–45. doi:10.1007/s100400050178.

Zaramella M, Marion A, Packman AI. 2006. Applicability of the Transient Storage

Model to the hyporheic exchange of metals. J Contam Hydrol. 84:21–35.

doi:10.1016/j.jconhyd.2005.12.002.

Figures

Figure 1. Lateral view of the hyporheic zone at the groundwater-surface water interface. Local variability in stream gradient and bedform (e.g., pools, riffles) can cause surface water to move in and out of the hyporheic zone via shallow hyporheic flow paths (solid blue lines). Downwelling zones on the head (upstream end) of the riffle have high dissolved oxygen, like the stream, whereas upwelling zones on the tail (downstream end) of the riffle are less oxygenated. Depending on the hydraulic pressure of the system, groundwater can flow up into the hyporheic zone ultimately into surface water via long flow paths (dashed blue lines). Adapted from Boulton 1993.

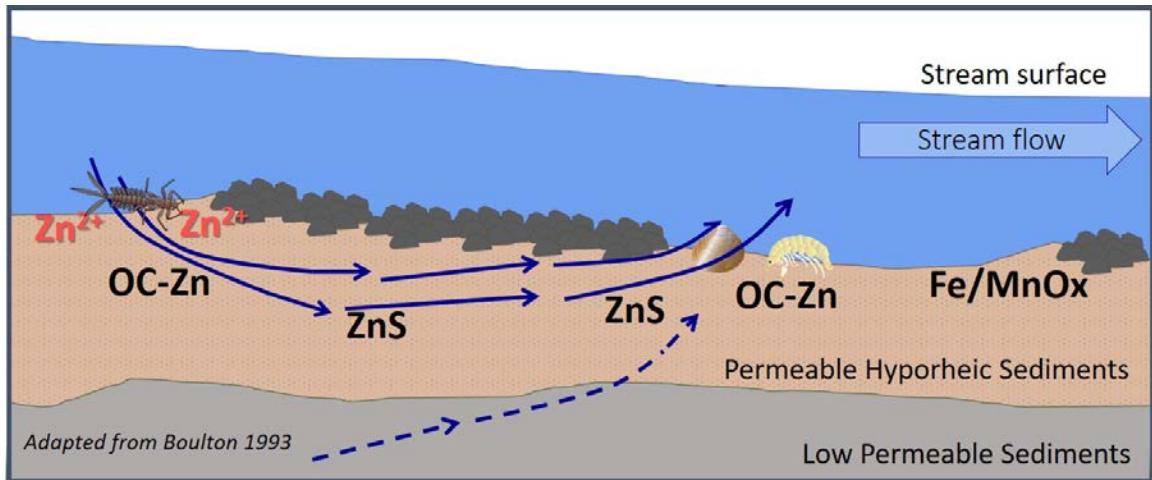


Figure 2. Lateral view of a singular experimental stream (flume). Each of the 12 experimental streams was set-up with the same surface and hyporheic flows. Six flumes contained reference sediments in both exposure baskets and six flumes contained Zn-spiked sediments in both baskets. Both the upstream sediment basket (non-hyporheic) and downstream basket (hyporheic) had three rhizon sampling ports, and porewater was extracted from ports r1 and r2.

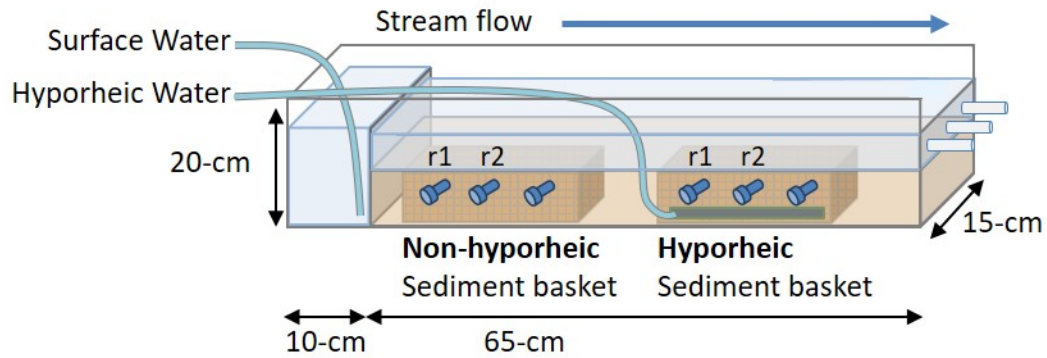


Figure 3. Temporal trends in porewater geochemistry during the initial experiment (left column; panels A, B, C) and aged experiment (right column; panels D, E, F). Time is in days on the x-axis and concentrations of porewater chemistry are on the y-axis. Graphs include: reduced iron (Fe^{2+}), dissolved oxygen (DO), and pH. Error bars denote ± 1 SE. Legend shortens Ref-nonHyp to “Ref” and Zn-nonHyp to “Zn”. A pH meter error on d9 of the aged experiment prevented pH measurements.

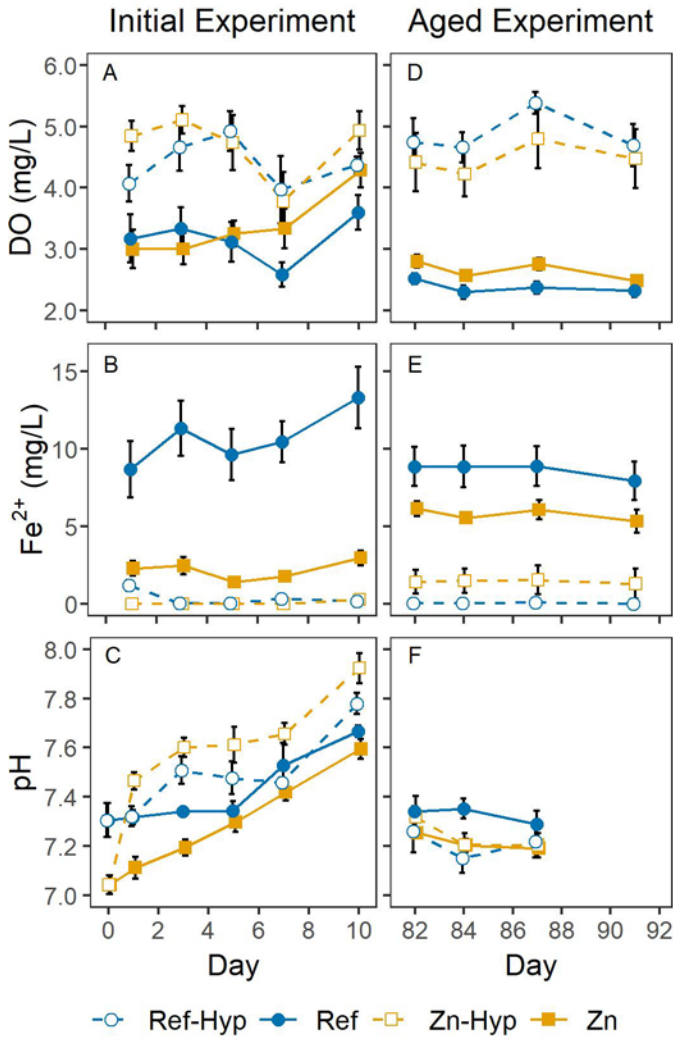


Figure 4. Temporal trends in porewater metal chemistry during the initial experiment (left column; panels A, B, C) and aged experiment (right column; panels D, E, F). Time is in days on the x-axis and concentrations of porewater metal are on the y-axis. Graphs include: porewater Fe, Mn and Zn. Error bars denote ± 1 SE. Legend shortens Ref-nonHyp to “Ref” and Zn-nonHyp to “Zn”.

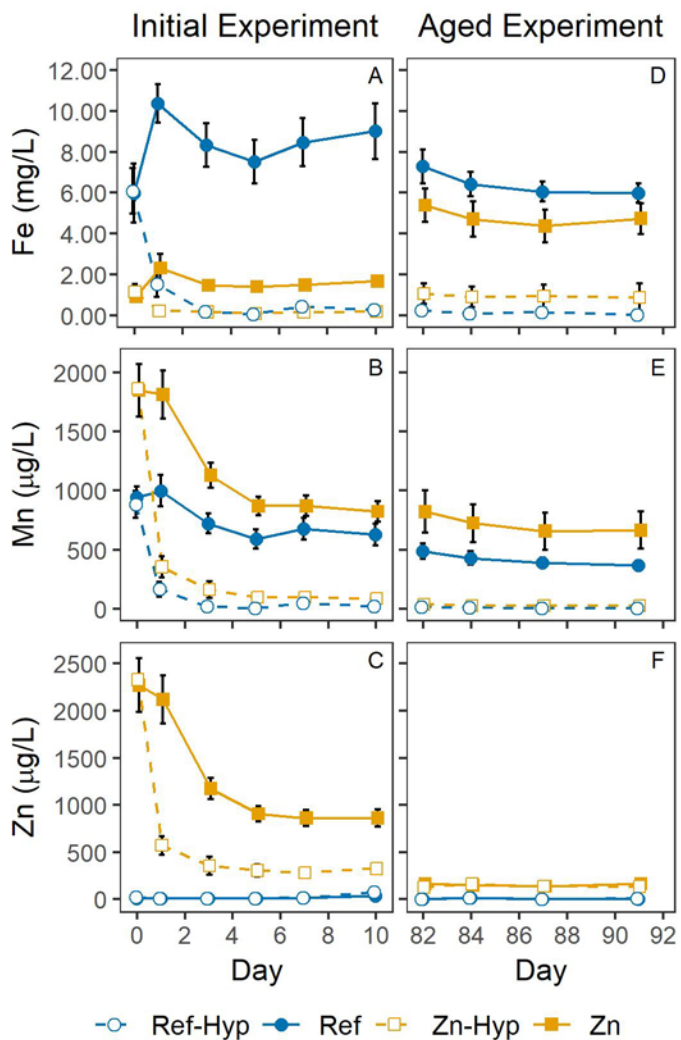


Figure 5. $(Zn_{SEM-AVS})/fOC$ (y-axis) did not differ between the Zn-nonHyp and Zn-Hyp exposures (x-axis) on day 10 of the initial experiment (panel A). On day 10 of the aged experiment, $(Zn_{SEM-AVS})/fOC$ was highest in Zn-Hyp exposure (panel B). Letters atop error bars denote differences in $(Zn_{SEM-AVS})/fOC$ among exposures within experiments.

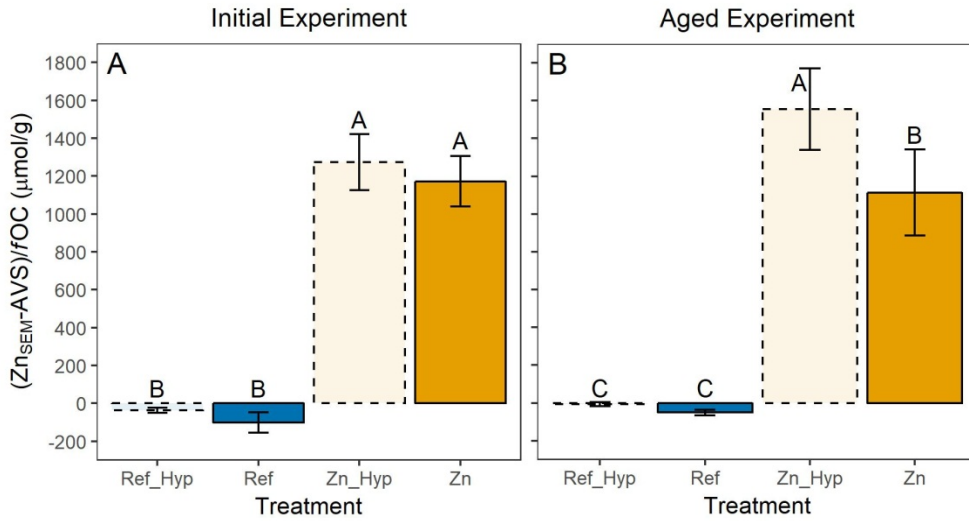
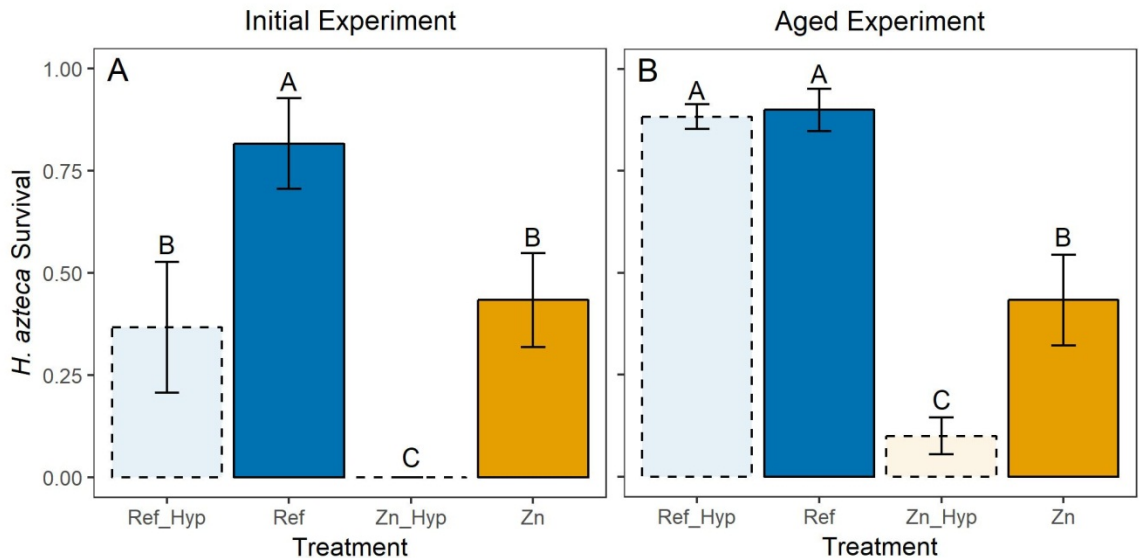


Figure 6. *H. azteca* survival (y-axis) in the initial (panel A) and aged (panel B) experiments was a function of sediment and hyporheic flow. Letters atop error bars denote differences in survival among exposures within experiments.



Tables

Table 1. Sediment chemical properties during the initial and aged experiments for: Reference (Ref) and Zinc-amended (Zn) sediments under hyporheic (Hyp) and non-hyporheic (nonHyp) flow treatments

Sediment-Hyporheic	Experiment	pH ^{a,b}	fOC ^c (% C)	AVS ($\mu\text{mol g}^{-1}$)	(SEM-AVS)/ fOC ($\mu\text{mol g}^{-1}$) ^c	Fe (g kg^{-1})	Mn (mg kg^{-1})	Zn (mg kg^{-1})
Reference	Pre-exposure	7.31	0.68	1.04	-139.1	5.4	42.1	7.6
Zinc	Pre-exposure	7.04	0.57	0.80	-33.3	3.8	37.7	425.9
Ref-nonHyp	Initial at d10	7.67 ± 0.02	1.28 ± 0.65	0.78 ± 0.25	-101.5 ± 132.0	5.11 ± 0.4	39.8 ± 2.7	7.0 ± 0.7
Ref-Hyp	Initial at d10	7.78 ± 0.04	0.71 ± 0.06	0.34 ± 0.10	-36.6 ± 34.2	5.44 ± 0.4	35.1 ± 2.4	8.2 ± 0.9
Zn-nonHyp	Initial at d10	7.60 ± 0.04	0.52 ± 0.09	0.56 ± 0.08	1172.4 ± 326.8	4.15 ± 0.1	36.4 ± 0.5	420.7 ± 11.8
Zn-Hyp	Initial at d10	7.92 ± 0.06	0.36 ± 0.04	0.36 ± 0.06	1272.6 ± 363.0	4.28 ± 0.2	28.2 ± 1.5	378.7 ± 17.5
Ref-nonHyp	Aged at d10	7.29 ± 0.06	0.68 ± 0.05	0.44 ± 0.14	-50.6 ± 29.8	6.21 ± 0.4	53.6 ± 3.7	15.5 ± 1.2
Ref-Hyp	Aged at d10	7.22 ± 0.06	1.10 ± 0.32	0.09 ± 0.09	-6.2 ± 20.8	7.12 ± 1.1	46.1 ± 5.4	15.4 ± 1.5
Zn-	Aged at	7.19 ±	0.53 ±	0.43 ±	1113.6 ±	4.42 ±	34.3 ±	405.9 ±

nonHyp	d10	0.05	0.13	0.04	457.6	0.4	3.2	30.4
Zn-Hyp	Aged at d10	7.20 ± 0.05	0.34 ± 0.01	0.44 ± 0.14	1555.5 ± 430.6	4.32 ± 0.2	29.1 ± 2.9	405.6 ± 24.6

^a pH was measured in the porewater

^b For pH, the aged experiment values are from day 5, not day 10

^c Loss-on-Ignition values were used to calculate *f*OC

*f*OC = fraction of organic carbon; AVS = Acid Volatile Sulfides; SEM = Simultaneously Extracted Metals; Fe = total sediment iron; Mn = total sediment manganese; Zn = total sediment zinc

Table 2. Initial experiment linear mixed effects model results for effects of time, hyporheic flow and Zn-amendment on porewater and sediment chemistry. The t-value and significance levels are reported, along with a (+) or (–) to indicate effects directions of main effects (i.e., positive or negative effect of time, hyporheic flow or Zn-spiked sediment)

Endpoints	Main Effects			Interactions		
	Time	Hyporheic	Zinc	Time*Hyp	Time*Zinc	Hyp*Zinc
Porewater DO	(+) 1.290	(+) 5.323***	(–) 0.036*	2.048*	0.905	0.226
Porewater Fe ²⁺ ^a	(–) 0.917	(–) 10.584***	(–) 5.296***	1.340	2.668**	0.362
Porewater pH	(+) 6.919***	(+) 0.832	(–) 4.655***	1.000	3.189**	5.618***
Porewater Fe ^a	(–) 0.179	(–) 6.755***	(–) 4.752***	2.987**	1.285	3.208**

Porewater Mn ^a	(-) 1.088	(-) 5.702***	(+) 1.347	3.369**	0.405	2.277*
Porewater Zn ^a	(+) 6.484***	(+) 1.045	(+) 27.111***	0.458	8.983***	4.920 ***
Total Fe	NA	(+) 0.846	(-) 3.020**	NA	NA	0.363
Total Mn	NA	(-) 1.851*	(-) 2.698*	NA	NA	0.954
Total Zn	NA	(+) 0.081	(+) 27.136***	NA	NA	2.234*
Zn _{SEM} -AVS/fOC	NA	(-) 0.609	(+) 9.796***	NA	NA	-0.235
Zn _{SEM}	NA	(-) 0.139	(+) 13.882***	NA	NA	2.700*
AVS	NA	(-) 2.358*	(+) 0.104	NA	NA	0.906
fOC	NA	(-) 1.328	(-) 0.821	NA	NA	0.672

^a Variables were log-transformed due to non-normal distributions

* $p < 0.1$; * $p < 0.05$; ** $p < 0.01$; *** $p < 0.001$

Zn_{SEM} = Zinc fraction of Simultaneously Extracted Metals; AVS = Acid Volatile Sulfides; fOC = fraction of Organic Carbon

Table 3. Aged experiment linear mixed effects model results for effects of time, hyporheic flow and Zn-amendment on porewater and sediment chemistry. The t-value and significance levels are reported, along with a (+) or (-) to indicate directions of main effects (i.e., positive or negative effect of time, hyporheic flow or Zn-spiked sediment)

Endpoints	Main Effects			Interactions		
	Time	Hyporheic	Zinc	Time*Hyp	Time*Zinc	Hyp*Zinc
Porewater DO	(-) 0.729	(+) 11.627***	(+) 0.929	1.161	0.017	3.053**
Porewater Fe ²⁺	(-) 1.481	(-) 19.429***	(-) 2.874*	1.187	0.012	8.163***
Porewater pH ^a	(-) 0.767	(-) 2.585*	(-) 1.611	0.139	0.658	2.960**
Porewater Fe	(-) 2.153*	(-) 17.238***	(-) 2.916**	1.297	0.576	5.883***
Porewater Mn ^b	(-) 1.588	(-) 24.869***	(+) 1.110	3.129**	0.755	3.357**
Porewater Zn ^b	(+) 0.864	(+) 0.007	(+) 11.021***	0.027	0.830	0.694
Total Fe	NA	(+) 1.159	(-) 3.545**	NA	NA	0.913
Total Mn	NA	(-) 1.477	(-) 3.382**	NA	NA	0.316
Total Zn	NA	(+) 0.002	(+) 15.424***	NA	NA	0.013
Zn _{SEM} -AVS/fOC	NA	(-) 0.751	(+) 8.105***	NA	NA	-4.760**
Zn _{SEM}	NA	(-) 0.077	(+) 10.363***	NA	NA	3.113*

AVS	NA	(-) 2.678*	(+) 2.504*	NA	NA	1.952*
fOC	NA	(+) 1.910*	(-) 3.250**	NA	NA	1.831*

^a Porewater pH was analyzed on days 82, 84 and 87; all other porewater analyses also included measurements on day 91

^b Variables were log-transformed due to non-normal distributions

* $p < 0.1$; * $p < 0.05$; ** $p < 0.01$; *** $p < 0.001$

Zn_{SEM} = Zinc fraction of Simultaneously Extracted Metals; AVS = Acid Volatile Sulfides; fOC = fraction of Organic Carbon